Selective P4 Activation by a Highly Reduced Cobaltate: Synthesis of Dicobalt Tetraphosphido Complexes

Pelties, S.; Maier, T.; Herrmann, D.; de Bruin, B.; Rebreyend, C.; Gaertner, S.; Shenderovich, I.G.; Wolf, R.

Link to publication

Citation for published version (APA):
Pelties, S., Maier, T., Herrmann, D., de Bruin, B., Rebreyend, C., Gaertner, S., Shenderovich, I. G., & Wolf, R. (2017). Selective P$_4$ Activation by a Highly Reduced Cobaltate: Synthesis of Dicobalt Tetraphosphido Complexes. *Chemistry-A European Journal*, *23*(25), 6094-6102. https://doi.org/10.1002/chem.201603296

■ Polyphosphides

Selective P$_4$ Activation by a Highly Reduced Cobaltate: Synthesis of Dicobalt Tetraphosphido Complexes

Stefan Pelties,[a] Thomas Maier,[a] Dirk Herrmann,[a] Bas de Bruin,[b] Christophe Rebreyend,[b] Stefanie Gärtner,[a] Ilya G. Shenderovich,[a] and Robert Wolf*[a]

Abstract: Although the chemistry of transition metal polyphosphide anions has attracted significant attention, there are few reports of studies in which such species have been synthesized directly from white phosphorus. [K(OEt$_2$)$_2${Co(BIAN)(cod)}] (**1**, BIAN = 1,2-bis(2,6-diisopropylphenylimino)acenaphthene, cod = 1,5-cyclooctadiene), which is readily prepared by ligand exchange from [K(thf)$_x${Co(cod)$_2$}], reacts with P$_4$ to afford [{K(thf)}$_2${(BIAN)Co}$_2$(μ-η^4:η^4-P$_4$)] (**2a**) in 61% yield (isolated product). [{K(OEt$_2$)}$_2${(BIAN)Co}$_2$(μ-η^4:η^4-P$_4$)] (**2b**) and [K([18]crown-6)(MeCN)]$_2$[{(BIAN)Co}$_2$(μ-η^4:η^4-P$_4$)] (**2c**) were obtained by recrystallizing **2a** from diethyl ether and aceto-

nitrile (and using [18]crown-6 in case of **2c**). Oxidation of **2a** with [Cp$_2$Fe]BAr$^F_4$ (one equivalent) and subsequent recrystallization of the product from different solvents gave [K(OEt$_2$){(BIAN)Co}$_2$(μ-η^4:η^4-P$_4$)] (**3a**) and [K(dme)$_4$][{(BIAN)Co}$_2$(μ-η^4:η^4-P$_4$)] (**3b**; dme = 1,2-dimethoxyethane). Neutral [{(BIAN)Co}$_2$(μ-η^4:η^4-P$_4$)] (**4**) was obtained in moderate yield by oxidizing **2a** with two equivalents of [Cp$_2$Fe]BAr$^F_4$. The new complexes were characterized by NMR, EPR (in the case of **3a**), and UV/Vis spectroscopy, and elemental analysis. The molecular structures revealed by X-ray crystallography display planar cyclic or open-chain P$_4^{4-}$ units sandwiched between {(BIAN)Co} fragments.

Introduction

Transition metal-mediated transformations are a potentially attractive approach for the efficient and environmentally benign activation of white phosphorus (P$_4$).[1] Subsequent reactions of the resulting polyphosphido complexes may give rise to interesting new polyphosphorus compounds and may contribute to the development of new, effective P$_4$ functionalization protocols.[2]

Traditionally, transition metal-containing polyphosphide anions have been prepared by reaction of alkali metal polyphosphides, for example, M$_3$P$_7$ (M = alkali metal), with transition metal carbonyls or transition metal halides,[3] or by reducing neutral polyphosphido complexes with electropositive metals, such as sodium, potassium, or lanthanoid complexes.[4–7] The synthesis of anionic cyclopentadienyl and β-diketiminato polyphosphorus compounds by reduction of neutral precursors has recently attracted particular attention.[5–7] The [Nb(ODipp)$_3$P$_3$]$^-$ anion (**A**, Dipp = 2,6-iPr$_2$C$_6$H$_3$; Figure 1),

prepared in one step by reducing [NbCl$_2$(OAr)$_3$(thf)] with Na/Hg in the presence of P$_4$, is a landmark example for reactive transition metal polyphosphide anions.[9] Anion **A** was used as a P$_3^{3-}$ transfer agent to synthesize elusive EP$_3$ molecules (E = As, Sb). Low-valent transition metallate anions can be used to activate P$_4$ directly, forming polyphosphide anions. However, this approach has rarely been exploited to date. Ellis and co-workers prepared the intriguing sandwich complex **B** (Figure 1) by treating [Ti(C$_{10}$H$_8$)$_3$]$^{2-}$ (C$_{10}$H$_8$ = naphthalene) with P$_4$.[10] We investigated the reactivity of the naphthalene ferrate [Cp*Fe(C$_{10}$H$_8$)]$^-$ with P$_4$.[11] A mixture of several structurally diverse products was formed, including the crystallographically characterized complexes **C** and **D** (Figure 1). This result shows the potential complexity of this type of transformation.

In extension of our previous studies, we sought to prepare new complex anions that are able to activate P$_4$ more selectively. Herein we report that the reaction of the new cobaltate complex [K(OEt$_2$)$_2${Co(BIAN)(cod)}] (**1**, cod = 1,5-cyclooctadiene) with P$_4$ affords the [{(BIAN)Co}$_2$(μ-η^4:η^4-P$_4$)]$^{2-}$ dianion, which we have isolated in the form of three potassium salts

[a] *Dr. S. Pelties, T. Maier, D. Herrmann, Dr. S. Gärtner, Dr. I. G. Shenderovich, Prof. Dr. R. Wolf*
Institute of Inorganic Chemistry, University of Regensburg
93040 Regensburg (Germany)
E-mail: robert.wolf@ur.de
Homepage: http://www.uni-regensburg.de/chemistry-pharmacy/inorganic-chemistry-wolf/index.html

[b] *Prof. Dr. B. de Bruin, C. Rebreyend*
Van 't Hoff Institute for Molecular Sciences, University of Amsterdam
Science Park 904, 9747 AG Groningen (Netherlands)

🖵 *Supporting information and ORCID(s) for the author(s) for this article is*
ⓘ *available on the WWW under http://dx.doi.org/10.1002/chem.201603296.*
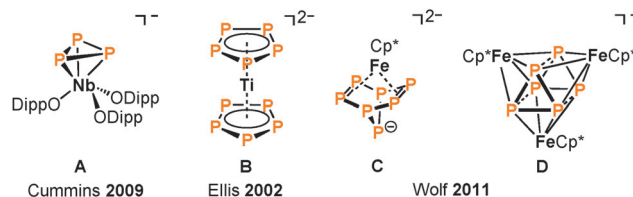
Figure 1. Anionic transition metal polyphosphido complexes directly obtained by P$_4$ activation. Cp* = C$_5$Me$_5$, Dipp = 2,6-iPr$_2$C$_6$H$_3$.[9–11]

[{K(thf)}₂{(BIAN)Co}₂(μ-η⁴:η⁴-P₄)] **(2 a)**, [{K(OEt₂)}₂{(BIAN)Co}₂-(μ-η⁴:η⁴-P₄)] **(2 b)**, and [K([18]crown-6)(MeCN)]₂[{(BIAN)Co}₂-(μ-η⁴:η⁴-P₄)] **(2 c)**. Targeted preparative oxidations led to [K(OEt₂){(BIAN)Co}₂(μ-η⁴:η⁴-P₄)] **(3 a)** and [K(dme)₄][{(BIAN)Co}₂-(μ-η⁴:η⁴-P₄)] **(3 b**; dme = 1,2-dimethoxyethane), containing the [(BIAN)Co}₂(μ-η⁴:η⁴-P₄)]⁻ monoanion, as well as neutral [{(BIAN)-Co}₂(μ-η⁴:η⁴-P₄)] **(4)**. We describe the single-crystal X-ray structures, and the NMR, EPR, and UV/Vis spectroscopic properties of these new complexes. Their molecular structures feature structurally distinct P₄⁴⁻ fragments with cyclic and open-chain arrangements. We discuss the influence of the redox-active bis-(imino)acenaphthene scaffold and compare our complexes with related β-diketiminato (nacnac) iron and cobalt compounds that were recently reported by the groups of Driess and Scheer.[7,8]

Results and Discussion

Reaction of one equivalent of BIAN with Jonas's complex [K(thf)₀.₂{Co(cod)₂}]][12] in THF at room temperature produces [K(OEt₂){Co(BIAN)(cod)}] **(1)** in 71% yield (isolated product) after crystallization from diethyl ether (Scheme 1). The reaction proceeds selectively according to ¹H NMR monitoring.[13] Dark green, almost black crystalline **1** is highly oxygen and moisture sensitive and dissolves well in polar solvents, such as diethyl ether and THF.
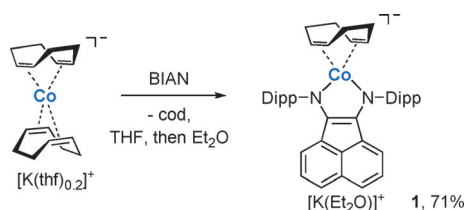
Scheme 1. Synthesis of **1**.

A single crystal X-ray diffraction (XRD) experiment revealed the molecular structure of **1** (Figure 2 a), which adopts a distorted square planar coordination environment for cobalt with a twist angle of 17.6°. The potassium cation is η⁴-coordinated by the planar α-diimine framework of the BIAN ligand and additionally by two THF molecules. The C1—N1 [1.380(3) Å], C2—N2 [1.382(3) Å], and C1—C2 [1.383(3) Å] bond lengths of the [Co(BIAN)(cod)]⁻ anion are equal within experimental error. The elongated C—N and shortened C—C bond lengths with respect to the free BIAN molecule indicate the presence of a BIAN²⁻ dianion (Figure 2 b).[14–17] It is noteworthy that the isoelectronic complex [Ni(BIAN)(cod)], synthesized by Stephan and co-workers, features a monoanionic BIAN⁻ framework (C—N 1.324–1.336 Å; C—C 1.426–1.428 Å).[17] The observation of a BIAN²⁻ dianion in **1** is likely attributed to the low effective nuclear charge and lower reduction potential of cobalt.

DFT optimization (B3LYP/def2-TZVP level, see the supporting information for details) of the closed-shell singlet state gave a close agreement between the computed structure and the crystallographically determined one. Optimizations of the
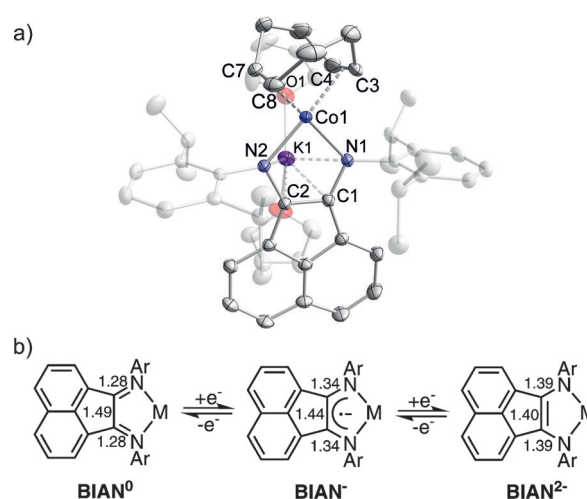
Figure 2. a) Solid-state molecular structure of [K(thf)₂{Co(BIAN)(cod)}] **(1)**. The hydrogen atoms are omitted for clarity. Thermal ellipsoids are drawn at the 40% probability level. Selected bond lengths [Å] and angles [°]: Co1—C3 2.029(2), Co1—C4 2.028(2), Co1—C7 2.050(2), Co1—C8 2.012(2), Co1—N1 1.953(2), Co1—N2 1.936(2), C1—N1 1.380(3), C2—N2 1.382(2), C1—C2 1.383(3), C3—C4 1.390(4), C7—C8 1.396(3); N1-Co1-N2 84.14(7). b) Average C—N and C—C bond lengths of different oxidation states of known BIAN complexes.[14–17]

open-shell singlet using the broken symmetry formalism converged at the closed-shell structure, indicating that this represents the ground state.

One set of ¹H NMR signals is observed for **1** in [D₈]THF for the BIAN fragment and coordinated cod. The latter gives rise to two multiplets at δ = 1.12 and 2.33 ppm for the diastereotopic methylene protons and another multiplet at δ = 2.91 ppm for the methine protons. Signals at δ = 32.6 and 64.1 ppm are observed in the ¹³C{¹H} NMR spectrum. [Co(cod)₂]⁻ gives rise to similar NMR shifts.[12] A cyclic voltammogram recorded in THF/[nBu₄N](PF₆) revealed a quasi-reversible one-electron oxidation process at a fairly negative potential of $E_{1/2} = -1.72$ V vs. Fc/Fc⁺ (see the Supporting Information, Figure S9), which presumably corresponds to the oxidation of **1** to give neutral [Co(BIAN)(cod)].[18] The UV/Vis spectrum of **1** in THF shows one intense absorption at λ = 289 nm, as well as two bands in the visible region at λ = 441 and 663 nm (see the Supporting Information, Figure S10). The absorption maximum of the latter band is shifted to λ = 485 nm in diethyl ether. This substantial change may indicate positive solvatochromism, a phenomenon that is typically observed for unsymmetrical ligand-to-ligand charge transfer (LL'CT) complexes.[19]

The reaction of **1** with white phosphorus gives [{K(thf)}₂{(BIAN)Co}₂(μ-η⁴:η⁴-P₄)] **(2 a**, Scheme 2) in 61% yield (isolated product). Monitoring by ¹H and ³¹P{¹H} NMR spectroscopy showed that the reaction is highly selective in THF at room temperature and proceeds to completion within several hours. Crystals of [{K(OEt₂)}₂{(BIAN)Co}₂(μ-η⁴:η⁴-P₄)] **(2 b)** suitable for single-crystal XRD were obtained by recrystallization from diethyl ether. The structure shows a centrosymmetric [{(BIAN)-Co}₂(μ-η⁴:η⁴-P₄)]²⁻ dianion with an inverted sandwich structure (Figure 3, top). The two potassium cations are each connected to two P atoms, one diethyl ether molecule, and the Dipp sub-

stituents. The salient feature of the structure is the rectangular P_4 unit located on the crystallographic inversion center. The P1—P2 bond length [2.161(1) Å] lies in the known range for aromatic P_4^{2-} anions, for example, that in Korber's tetraphosphide $Cs_2P_4 \cdot 2NH_3$ [P—P 2.146(1) and 2.1484(9) Å].[20–22] P1—P2′ [2.500(1) Å] is much longer than a typical P—P single bond, but shorter than a van der Waals contact.[4b, 22, 23]

According to these structural parameters, a superposition I↔II of two resonance structures (see below, Figure 9a), comprising two P_2^{2-} dianions (I) and a P_4^{4-} unit (II), appears to be an apt description of the structural and electronic situation. Assuming the presence of monoanionic BIAN⁻ ligands, as indicated by the structural parameters [C1—N1 1.348(2), C2—N2 1.343(4), C1—C2 1.404(4) Å],[14–17] this would result in the two cobalt atoms having the +II oxidation state.

To probe whether the potassium ions influence the shape of the Co_2P_4 core,[24] [K([18]crown-6)(MeCN)]₂[{(BIAN)Co}₂(μ-η⁴:η⁴-P_4)] (2c) with an ion-separated structure was synthesized by recrystallizing 2a from acetonitrile in the presence of two equivalents of [18]crown-6. The potassium cations do not interact with the anion in the crystal structure (see the Supporting Information, Figure S7). The anion of 2c is similar to 2b, but shows slightly shorter P—P bond lengths in the P_2^{2-} units [P1—P2 2.0862(6) Å, that is, 0.075 Å shorter than in 2b], and a slightly longer separation between these units [P1—P2′ 2.5523(6) Å, elongated by 0.052 Å compared to 2b].
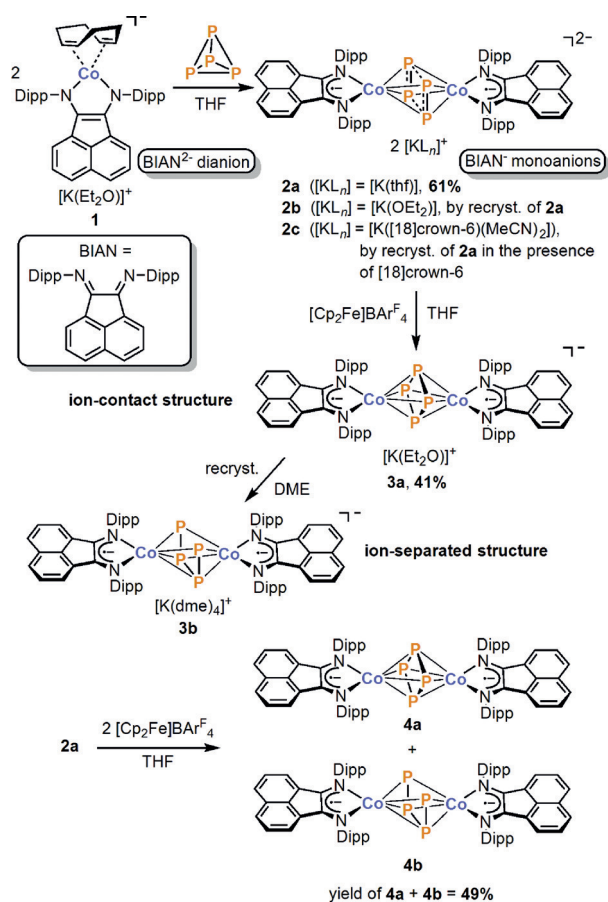

Scheme 2. Synthesis of new dicobalt tetraphosphido complexes 2–4.
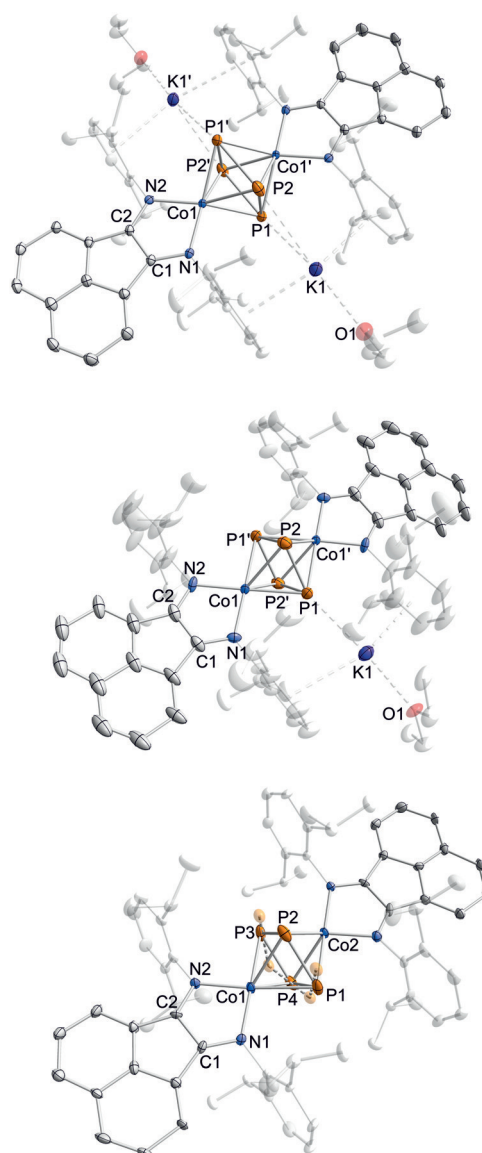
Figure 3. Solid-state molecular structures of [{K(OEt₂)}₂{(BIAN)Co}₂(μ-η⁴:η⁴-P_4)] (2b, top), [K(OEt₂){(BIAN)Co}₂(μ-η⁴:η⁴-P_4)] (3a, center) and [{(BIAN)Co}₂(μ-η⁴:η⁴-P_4)] (4, bottom). The hydrogen atoms are omitted for clarity. Thermal ellipsoids are drawn at the 40% probability level. Selected bond lengths [Å] and angles [°] for 2b: Co1—Co1′ 3.2733(9), P1—P2 2.161(1), P1—P2′ 2.500(1), Co1—P1 2.3209(9), Co1—P2 2.3342(9), Co1—P1′ 2.3195(9), Co1—P2′ 2.3285(9), Co1—N1 1.930(2), Co1—N2 1.932(2), C1—N1 1.348(2), C2—N2 1.343(4), C1—C2 1.404(4); P1-P2-P1′ 89.45(4), P2-P1′-P2′ 90.55(4), N1-Co1-N2 83.32(9); 3a: Co1—Co1′ 3.469(3), P1—P2 2.224(4), P1—P2′ 2.226(4), Co1—P1 2.309(3), Co1—P2 2.367(3), Co1—P1′ 2.315(3), Co1—P2′ 2.375(3), Co1—N1 1.938(7), Co1—N2 1.919(7), C1—N1 1.32(1), C2—N2 1.32(1), C1—C2 1.44(1); P1-P2-P1′ 86.8(1), P2-P1′-P2′ 93.2(1), N1-Co1-N2 82.2(3); 4a (major component): Co1—Co2 3.3807(4), P1—P2 2.215(3), P2—P3 2.274(2), P3—P4 2.202(3), P4—P1 2.268(2), Co1—P1 2.310(2), Co1—P2 2.345(2), Co1—N1 1.914(1), Co1—N2 1.913(1), C1—N1 1.344(5), C2—N2 1.336(5), C1—C2 1.444(6); P1-P2-P3 89.7(1), P2-P3-P4 90.17(8), N1-Co1-N2 84.2(2); 4b (minor component): P1A—P2A 2.36(1), P2A—P3A 2.17(1), P3A—P4A 2.34(2), P4A—P1A 3.18(2); P1A-P2A-P3A 104.2(4), P2A-P3A-P4A 100.2(5).

The cyclic voltammogram of 2a recorded in THF/[nBu₄N](PF₆) features two reversible one-electron oxidation processes at $E_{1/2} = -1.98$ V and -1.26 V vs. Fc/Fc⁺, and an irreversible two-electron oxidation wave at $E_{pa} = -0.43$ V vs. Fc/
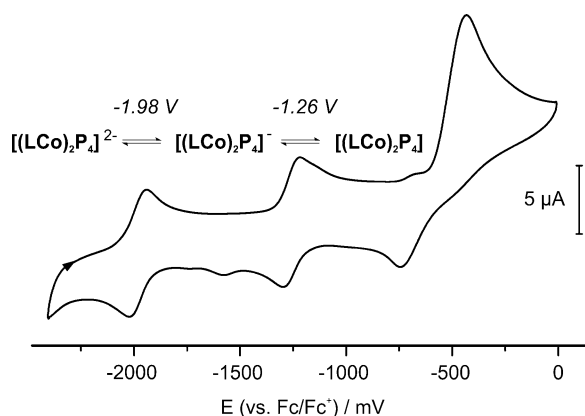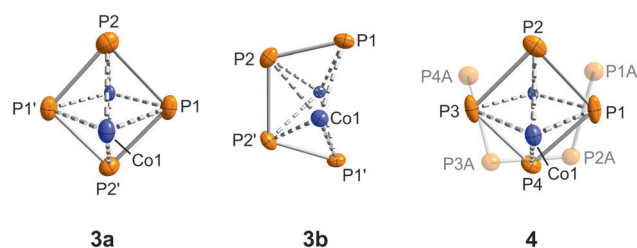
Figure 4. Cyclic voltammogram of **2a** recorded in THF/[nBu_4N]PF$_6$ with a platinum disc working electrode, a platinum wire as counter electrode, and a silver wire as pseudoreference electrode. $v = 100\ mV\,s^{-1}$; potentials are referenced to the Fc/Fc$^+$ couple; L = BIAN.

Figure 5. The Co$_2$P$_4$ cores shown along the Co-Co axis in the molecular structures of **3a**, **3b**, and **4**. Thermal ellipsoids are drawn at the 40% probability level. Selected bond lengths [Å] and angles [°] of **3a**: Co1–Co1′ 3.469(3), P1–P2 2.224(4), P1–P2′ 2.226(4); P1-P2-P1′ 86.8(1), P2-P1′-P2′ 93.2(1), N1-Co1-N2 82.2(3); **3b**: Co1–Co1′ 2.8455(5), P1–P2 2.0631(5), P2–P2′ 2.3912(8), P1–P1′ 3.418(2), P1-P2-P2′ 104.411(5); **4a** (major component): Co1–Co2 3.3807(4), P1–P2 2.215(3), P2–P3 2.274(2), P3–P4 2.202(3), P4–P1 2.268(2); P1-P2-P3 89.7(1), P2-P3-P4 90.17(8); **4b** (minor component, transparent P atoms): P1A–P2A 2.36(1), P2A–P3A 2.17(1), P3A–P4A 2.34(2), P4A–P1A 3.18(2); P1A-P2A-P3A 104.2(4), P2A-P3A-P4A 100.2(5).

Fc$^+$ (Figure 4).[25] Additional weak irreversible waves at $E_{pa} = -0.66\ V$ and $E_{pc} = -1.58\ V$ presumably arise from secondary redox processes of the products formed by the irreversible oxidation event.

Stimulated by these promising CV data, we synthesized the monopotassium salt [K(OEt$_2$){(BIAN)Co}$_2$(μ-η^4:η^4-P$_4$)] (**3a**) and the neutral complex [{(BIAN)Co}$_2$(μ-η^4:η^4-P$_4$)] (**4**) on a preparative scale by treating **2a** with [Cp$_2$Fe]BAr$^F_4$ (one and two equivalents, respectively) in THF (Scheme 2). Chemical oxidation of **2a** with an excess of [Cp$_2$Fe]BF$_4$ (eight equivalents) afforded free P$_4$ as the only species detected in the ^{31}P{^{1}H} NMR spectrum in [D$_8$]THF. Using six equivalents of the ferrocenium salt, a mixture of P$_4$, **4**, and an unidentified minor species showing a singlet at $\delta = 205.5$ ppm was formed in a 65:30:5 ratio according to ^{31}P NMR integration.

Single-crystal XRD on **3a** (Figures 3 and 5) revealed a similar overall arrangement as for **2b** and **2c**. However, the structure of the central P$_4$ moiety is different, showing a rhombic arrangement [P1-P2-P1′ 86.8(1), P2-P1′-P2′ 93.2(1)°] with P–P single bonds [2.224(4) and 2.264(4) Å] throughout the ring. These data indicate the presence of a cyclo-P$_4^{4-}$ ligand (resonance structure **II**, Figure 9a), a framework that was previously only observed for some Zr, Nb, and Ta complexes.[3, 22] Inspection of the C–N and C–C distances [C1–N1 1.32(1), C2–N2 1.32(1), C1–C2 1.44(1) Å] indicates that monoanionic BIAN$^-$ anions are present with little back-bonding of the metal.[17] Compared to **2b**, the Co–Co distance increases by 0.2 Å [Co1–Co1′ 3.469(3) Å, cf. 3.2733(9) Å in **2b**]. The potassium ion is disordered over two positions and has the same ligand environment as in **2b**.

Complex **3a** is paramagnetic. The solution effective magnetic moment [2.0(1) μ$_B$] determined in [D$_8$]THF indicates the presence of one unpaired electron per molecule. As a consequence of its paramagnetic nature, broad ^{1}H NMR signals are observed in the range of −0.9 to 19.3 ppm. The X-band EPR spectrum of **3a** (Figure 6) recorded in THF (ca. 0.1 M [nBu_4N](PF$_6$) added to obtain a better glass) reveals a rhombic signal with cobalt hyperfine interactions characteristic for an $S = \frac{1}{2}$ system. A

decent simulation of the experimental spectrum was obtained assuming a hyperfine interaction (HFI) with two equivalent cobalt nuclei (g$_x$ = 2.127, g$_y$ = 2.081, g$_z$ = 2.008; A$_x^{Co}$ = 50 MHz, A$_y^{Co}$ = 200 MHz, A$_z^{Co}$ = 240 MHz). Other HFIs are not resolved, indicating that the unpaired electron is primarily delocalized over the two cobalt atoms.
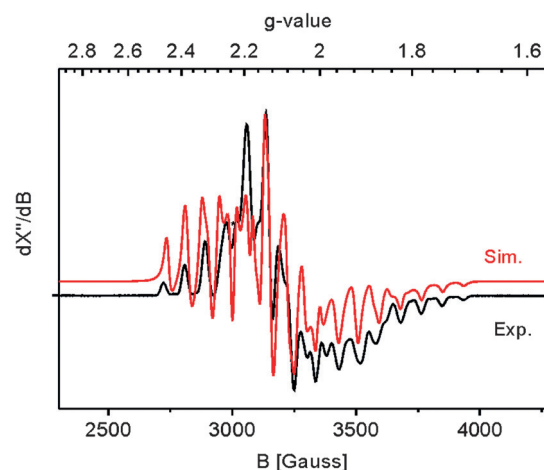
Figure 6. Experimental and simulated X-band EPR spectrum of **3a** recorded in THF (ca. 0.1 M [nBu_4N](PF$_6$) added to obtain a better glass). Experimental parameters: microwave frequency 9.385050 GHz; microwave power 0.2 mW; mod. ampl 4 G. The simulation was obtained by using the following parameters: g$_x$ = 2.127, g$_y$ = 2.081, g$_z$ = 2.008; A$_x^{Co}$ = 50, A$_y^{Co}$ = 200, A$_z^{Co}$ = 240 MHz (two equivalent cobalt nuclei; I = 7/2).

The ion-separated structure **3b** was obtained by recrystallizing a sample of **3a** from 1,2-dimethoxyethane (DME). The single-crystal XRD analysis (see the Supporting Information, Figure S8) shows that, in contrast to **3a**, the Co$_2$P$_4$ core of **3b** (Figure 5) features an open-chain tetraphosphabutadiene fragment (**III**, Figure 9a) with double bonds between the terminal phosphorus atoms [P1=P2 2.0631(5) Å] and an elongated single bond between the internal P atoms [P2–P2′ 2.3912(8) Å]. The large distance between the terminal P atoms [P1–P1′ 3.418(2) Å] indicates the absence of a P–P bond.

The neutral compound [(BIAN)Co}$_2$(μ-η^4:η^4-P$_4$)] (**4**) was obtained in 49% yield by oxidizing **2a** with two equivalents of [Cp$_2$Fe]BAr$^F_4$. The solid-state molecular structure is disordered (Figure 3 and 5) and consists of two components, a major component **4a** (91% occupancy) and a minor one **4b** (9% occupancy). **4a** includes a rectangular, almost square-like, cyclo-P$_4^{4-}$ ligand [P1-P2-P3 89.7(1), P2-P3-P4 90.17(8)°] with P—P bond lengths [2.202(3)–2.274(2) Å] similar to those in monoanionic **3a**. The C—N and C—C distances [C1—N1 1.344(5), C2—N2 1.336(5), C1—C2 1.444(6) Å] indicate the presence of BIAN$^-$ monoanions.[14–17] The Co—Co distance of 3.3807(4) Å is slightly shorter than in **3a**. The minor component **4b** includes a different P$_4$ fragment, which clearly has an open-chain structure similar to that observed in **3b** (**III**, Figure 9a). The low occupancy of this fragment leads to some uncertainty in the P—P distances, although the basic structural motif is unambiguous. Hence, it is difficult to decide whether a P$_4^{4-}$ tetraanion or a P$_4^{2-}$ dianion is present in **3b**.[26]

Diamagnetic **4** gives rise to one set of ^{1}H NMR signals in deuterated toluene; in addition, traces of the starting material **3a** are detected (see the Supporting Information, Figure S5), which cannot be removed completely by recrystallization. The ^{31}P{^{1}H} NMR spectrum of **4** (Figure 7) shows distinct singlets at $\delta = 253.9$ and 249.7 ppm in a 10:1 ratio. It is plausible that these signals correspond to the major and minor components **4a** and **4b** observed in the single-crystal X-ray structure (vide supra). A variable temperature ^{31}P{^{1}H} NMR experiment showed only minor changes in the temperature range of −80 to 100 °C (see the Supporting Information, Figure S6); coalescence of the two signals was not observed. Similarly, ^{31}P–^{31}P EXSY spectra did not reveal any cross peaks between the two signals. These observations support the notion that **4a** and **4b** do not exchange in solution.[26]
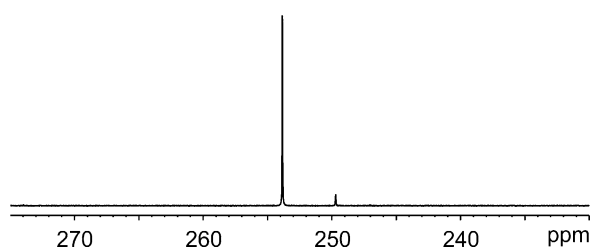

Figure 7. ^{31}P{^{1}H} NMR spectrum of **4** in [D$_8$]toluene at room temperature.

Figure 8a shows the ^{31}P MAS NMR spectrum of polycrystalline **4**. The simulation of the experimental spectrum demonstrates that there are two sets of overlapping signals. Both resonances are characterized by fast relaxation and a large linewidth. The dominant signal at $\delta = 256$ ppm exhibits a large chemical shift anisotropy. The intensity of the minor signal at $\delta = 245$ ppm is about 5% that of the major species. This signal does not exhibit any measurable chemical shift anisotropy, which might be tentatively attributed to the presence of dynamics on the millisecond or shorter timescale. Taking into account the results of the solution NMR and XRD investigations,
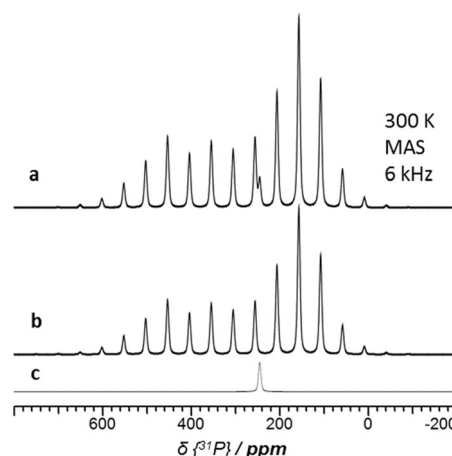

Figure 8. MAS (6 kHz) ^{31}P NMR spectrum of **4** at 300 K: a) Experimental spectrum; b) simulated spectrum ($\delta_{iso} = 256.0$ ppm, $\delta_{11} = 580$ ppm, $\delta_{22} = 130$ ppm, $\delta_{33} = 60$ ppm, linewidth ≈ 700 Hz); c) simulated spectrum ($\delta_{iso} = 245.0$ ppm, linewidth ≈ 900 Hz).

the dominant signal should be attributed to **4a** and the minor one to **4b**.

The electronic spectra of **2**–**4** in THF (see the Supporting Information, Figure S11) show medium intense bands in the NIR range at $\lambda = 795$ and 1135 nm (for **2a**), 777 and 1319 nm (for **3a**), and 884 nm (for **4**). These low-energy bands presumably arise from LL'CT transitions. The spectra feature additional intense absorptions in the UV and visible regions [**2a** and **2c**: 345 and 585 nm; **3a** and **3b**: 342 and 575 nm; **4**: 336, 427, 547, and 693 nm]. The UV/Vis spectrum of **2c** is identical to that of **2a**, while **3b** gives the same spectrum as **3a**, despite the compounds having an ion-contact structure vs. an ion-separated structure in the solid state. **2a** and **2c** give rise to singlets at $\delta = -45.9$ ppm for **2a** and $\delta = -44.0$ ppm for **2c** in the ^{31}P{^{1}H} NMR spectra recorded in [D$_7$]DMF. The similar electronic spectra and chemical shifts indicate similar structures for these compounds in solution.
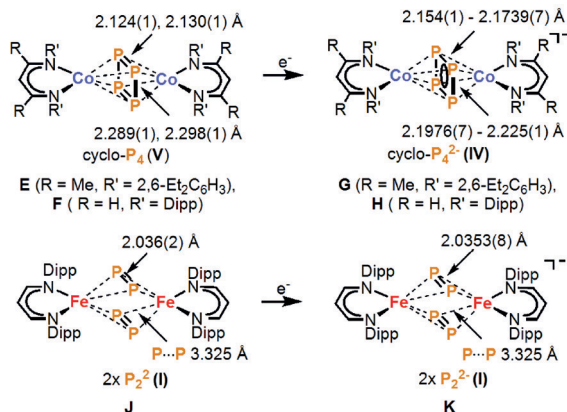
Comparing the molecular structures of **2**–**4** (Figure 9), we can conclude that an oxidation or reduction of the whole complex apparently hardly affects the oxidation state of the P$_4^{4-}$ fragment. Thus, according to the structural data, the electronic structure of **2b** and **2c** may be described as a superposition of two mesomeric forms **I**↔**II**. Resonance form **I** comprises two separated P$_2^{2-}$ units (**I**, Figure 9a,b), whereas **II** represents a P$_4^{4-}$ ring. The solid-state structures of mixed-valence **3a** and **3b** feature a rhombic cyclo-P$_4^{4-}$ and a chain-like catena-P$_4^{4-}$ fragment, respectively. The oxidation **2a**→**3a/b** thus appears to be a metal-centered redox process; the oxidation state of the tetraphosphorus fragment remains the same. Remarkably, even neutral **4**, obtained by two-electron oxidation of **2a** features a cyclo-P$_4^{4-}$ unit for the major component **4a** of the disordered structure. The oxidation state of the catena-P$_4^{x-}$ unit of the minor species **4b** is uncertain.[26] To summarize, the P$_4^{4-}$ ligand undergoes remarkable structural transformations, but retains its highly reduced tetraanionic character in the neutral, anionic, and dianionic forms of the complex. Nonetheless, its structure appears to be very sensitive to subtle changes in the
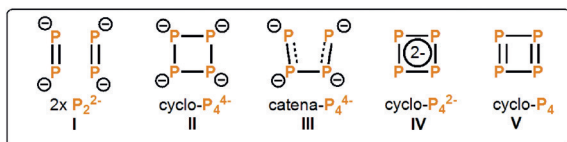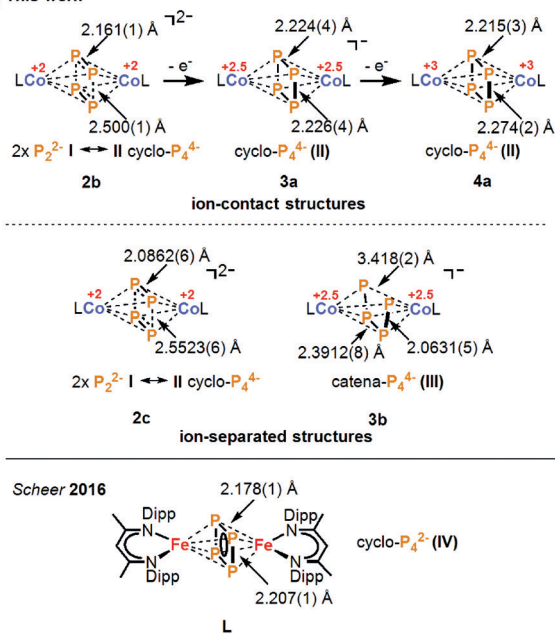
Figure 9. a) Schematic representation of possible structures for a planar P_4 framework; b) summary of structural data of BIAN complexes **2–4** (L = BIAN); c) summarized structural data of β-diketiminato complexes **E–M** prepared by the groups of Driess and Scheer.[7,8]

oxidation state of the cobalt atoms and the presence of differently solvated potassium countercations. Similar observations were previously made for cyclopentadienyl complexes [$Cp^R{}_2M_2P_4$] (Cp^R = substituted cyclopentadienyl ligand, M = Fe and Co), where the substitution pattern on the cyclopentadienyl ligand has a profound effect on the structures of the $P_4{}^{x-}$ fragment.[23b,28]

Furthermore, the structures of **2–4** can be distinguished from related β-diketiminato iron and cobalt complexes **E–L** (Figure 9) recently reported by the groups of Driess and Scheer.[7,8] Driess and co-workers prepared [{(nacnac^1)Co}$_2$(μ-η^4:η^4-P$_4$)]$^-$ (**G**, nacnac^1 = CH[CMeN(2,6-Et$_2$C$_6$H$_3$)]$_2$), [{(nacnac^2)Co}$_2$(μ-η^4:η^4-P$_4$)]$^-$ (**H**, nacnac^2 = CH[CHN(2,6-iPr$_2$C$_6$H$_3$)]$_2$), and [{(nacnac^2)Fe}$_2$(μ-η^2:η^2-P$_2$)$_2$]$^-$ (**K**) by reducing the neutral precursors **E**, **F**, and **J** (Figure 9 c).[7] Scheer and co-workers compared the steric influence of different nacnac ligands in related neutral species [{(nacnac^3)Fe}$_2$(μ-η^4:η^4-P$_4$)] (**L**, Figure 9 c, nacnac^3 = CH[CMeN(2,6-iPr$_2$C$_6$H$_3$)]$_2$), [{(nacnac^4)Fe}$_4$(μ$_4$-η^2:η^2:η^2:η^2-P$_8$)] (**M**, nacnac^4 = CH[CMeN(2,6-Me$_2$C$_6$H$_3$)]$_2$), and [{(nacnac^5)Fe}$_4$(μ$_4$-η^2:η^2:η^2:η^2-P$_8$)] (**N**, nacnac^5 = CH[CHN(2,6-Me$_2$C$_6$H$_3$)]$_2$).[8] The Co$_2$P$_4$ complexes **E** and **F** feature an unusual *neutral* cyclo-P$_4$ ligand (Figure 9 c, **V**), which transforms into a cyclo-P$_4{}^{2-}$ dianion (**IV**) upon one-electron reduction to afford **G** and **H**, respectively. Notably, **3 a** and **3 b** are isoelectronic with the Co$_2$P$_4$ complexes **G** and **H**. Whereas the latter feature a dianionic P$_4{}^{2-}$ framework, the more strongly electron-donating {(BIAN)Co} units apparently induce the presence of a tetraanionic P$_4{}^{4-}$ moiety in **3 a** as well as **3 b** and even in **4 a** (see above). The Fe$_2$P$_4$ species **J** and **K** include non-interacting P$_2{}^{2-}$ units (**I**, Figure 9 a), whereas closely related **L**, with more sterically encumbering Dipp substituents, features a cyclo-P$_4{}^{2-}$ dia-

nion (**III**) very similar to that in the cobalt compounds **G** and **H**. In contrast to **E–L**, the Fe$_4$P$_8$ complexes **M** and **N** (not shown in Figure 9) bear smaller 2,6-dimethylphenyl substituents. As a result, they have a tetranuclear structure where a P$_8{}^{4-}$ ligand with a realgar-like structure coordinates to four {(nacnac)Fe} fragments.[8] Subtle differences in the steric interaction of the ligand substituents thus appear to strongly affect the oxidation state of the central P$_4$ unit and the structure of the Fe$_2$P$_4$ core.

Conclusion

New dinuclear cobalt tetraphosphido complexes [{(BIAN)Co}$_2$(μ-P$_4$)]^x ($x = 0$, 1–, 2–) were obtained in three different oxidation states by treating the complex anion [K(OEt$_2$){Co(BIAN)(cod)}] (**1**) with P$_4$ and subsequent preparative oxidation of the reaction product [{K(thf)}$_2${(BIAN)Co}$_2$(μ-η^4:η^4-P$_4$)] (**2 a**). The molecular structures of the resulting complexes feature a P$_4{}^{4-}$ framework.[25] Its structure is significantly influenced by oxidation and reduction, as well as by coordination by the potassium cation. Thus, a cyclic P$_4{}^{4-}$ moiety is found in the molecular structures of **3 a** and **4 a**, whereas an open-chain P$_4{}^{4-}$ unit is observed in **3 b**. The use of the redox-active BIAN ligand appears crucial for achieving a high degree of P$_4$ reduction.[25,29] This observation underlines the exceptional electron-releasing and -accepting properties of the Co(BIAN) moiety. The subsequent reactivity of tetraphosphido complexes **2–4** is currently under investigation. Beyond P$_4$ activation, the reactivity of **1** and related complexes is being pursued, including potential catalytic applications.

Experimental Section

General procedures and starting materials

All experiments were performed under an atmosphere of dry argon using standard Schlenk techniques or an MBraun UniLab glovebox. Solvents were dried and degassed with an MBraun SPS800 solvent-purification system. Tetrahydrofuran and toluene were stored over molecular sieves (3 Å). Diethyl ether and *n*-hexane were stored over a potassium mirror. NMR spectra in solutions were recorded on Bruker Avance 300 and Avance 400 spectrometers at 300 K, if not stated otherwise, and internally referenced to residual solvent resonances. The solid-state ^{31}P NMR measurement was performed on an *Infinity*$_{plus}$ spectrometer (Agilent) operated at 7 Tesla, equipped with a 6 mm pencil CPMAS probe. The spectrum was indirectly referenced to H_3PO_4 (85% in H_2O). The experimental X-band EPR spectrum of **3a** was recorded on a Bruker EMX spectrometer (Bruker BioSpin Rheinstetten) equipped with a He temperature-control cryostat system (Oxford Instruments). Simulations of the EPR spectra were performed by iteration of the anisotropic g- values and linewidths by using the EPR simulation program W95EPR, available on request from Prof. F. Neese (MPI CEC Mülheim a/d Ruhr). Melting points were measured on samples in sealed capillaries on a Stuart SMP10 melting-point apparatus. UV/Vis spectra were recorded on a Varian Cary 50 spectrophotometer. NIR spectra were recorded on a Bruins Instruments Omega 20 spectrometer. Elemental analyses were carried out by the analytical department of Regensburg University. The starting materials [K(thf)$_{0.2}${Co(1,5-cod)$_2$}][12] and BIAN[14c] were prepared according to previously reported procedures.

Synthesis

1: A solution of BIAN (1.005 g, 2.01 mmol, 1.0 equiv) in THF (70 mL) was added to a solution of [K(thf)$_{0.2}${Co(1,5-cod)$_2$}] (660 mg, 2.01 mmol, 1.0 equiv) in THF (10 mL). An immediate color change to dark green was observed. After stirring the reaction mixture for two hours, the solvent was removed and the residue was taken up in diethyl ether (200 mL). Insoluble material was removed by filtration and the filtrate was concentrated to 75 mL and stored at room temperature. Dark green microcrystals of **1** formed upon storing for one day. Crystals suitable for X-ray diffraction were obtained by diffusion of *n*-hexane into a concentrated THF solution of **1**. The compound contained a variable amount of THF molecules after drying in high vacuum, which could be determined by ^{1}H NMR spectroscopy and elemental analysis. Yield 1.116 g (71%); m.p. > 230°C (decomp. to a black oil); ^{1}H NMR ([D$_8$]THF, 300 K, 400.13 MHz): $\delta = 0.96$ (br m, 12 H, CH(CH_3)$_2$), 1.12 (br m, 10 H, Et$_2$O/cod-CH$_2$), 1.38 (br m, 12 H, CH(CH_3)$_2$), 2.33 (br m, 4 H, cod-CH$_2$), 2.91 (br m, 4 H, cod-CH), 4.50 (br m, 4 H, CH(CH$_3$)$_2$), 4.89 (br m, 2 H, CH$_{BIAN}$), 6.20 (br m, 2 H, CH$_{BIAN}$), 6.28 (br m, 2 H, CH$_{BIAN}$), 7.00–7.09 ppm (br m, 6 H, *m-/p*-CH$_{Dipp}$); ^{1}H NMR ([D$_8$]THF, 333 K, 400.13 MHz) $\delta = 0.96$–0.99 (br m, 16 H, CH(CH_3)$_2$/cod-CH$_2$), 1.41 (d, ^3J(H,H) = 6.6 Hz, 12 H, CH(CH_3)$_2$), 2.34 (br m, 4 H, cod-CH$_2$), 2.90 (br m, 4 H, cod-CH), 4.48 (sept., ^3J(H,H) = 6.6 Hz, 4 H, CH(CH$_3$)$_2$), 5.01 (d, ^3J(H,H) = 6.3 Hz, 2 H, CH$_{BIAN}$), 6.28 (t, ^3J(H,H) = 7.7 Hz, 2 H, CH$_{BIAN}$), 6.34 (t, ^3J(H,H) = 7.7 Hz, CH$_{BIAN}$), 7.01–7.08 ppm (br m, 6 H, *m-/p*-CH$_{Dipp}$); ^{13}C{^{1}H} NMR ([D$_8$]THF, 300 K, 100.61 MHz) $\delta = 24.9$ (CH(CH_3)$_2$), 25.4 (CH(CH_3)$_2$), 28.1 (CH(CH$_3$)$_2$), 32.6 (cod-CH$_2$), 64.1 (cod-CH), 114.3 (CH$_{BIAN}$), 118.6 (CH$_{BIAN}$), 122.7 (CH$_{Dipp}$), 122.9 (CH$_{Dipp}$), 127.3 (CH$_{BIAN}$), 127.5 (C$_{BIAN}$), 135.8 (C$_{BIAN}$) 137.8 (C$_{BIAN}$), 143.5 (C$_{BIAN}$), 145.2 (*o*-CH$_{Dipp}$), 154.8 ppm (*ipso*-CH$_{Dipp}$); UV/Vis (THF): λ_{max} (ε) = 289 (26 000), 441 (12 000), 663 nm (8500 L mol^{-1} cm^{-1}); UV/Vis (Et$_2$O): λ_{max} (ε) = 284 (24 000), 436 (8500), 485 nm (9000 L mol^{-1} cm^{-1}); ele-

mental analysis calcd for C$_{52}$H$_{72}$N$_2$CoKO$_2$ (855.19): C 73.03, H 8.49, N 3.28; found: C 73.32, H 7.59, N 3.59.

2a, **2b**, and **2c**: P$_4$ (26 mg, 0.21 mmol, 1.0 equiv) was added at room temperature to a solution of **1** (328 mg, 0.420 mmol, 2.0 equiv) in THF (10 mL). After stirring the resulting violet reaction mixture for one day, the solution was filtered and the solid removed by filtration further taken up in THF (2 mL). The combined filtrates were concentrated to approximately 7 mL and layered with diethyl ether (ca. 25 mL). Dark microcrystals of [{K(thf)}$_2${(BIAN)Co}$_2$(μ-η^4:η^4-P$_4$)] (**2a**) formed upon storing the solution for one week at room temperature. Isolated **2a** contained approximately two THF molecules per formula unit after drying under high vacuum, as determined by ^{1}H NMR spectroscopy and elemental analysis. Yield 188 mg (61%); ^{1}H NMR ([D$_7$]DMF, 300 K, 400.13 MHz) $\delta = 0.78$ (br m, 24 H, CH(CH_3)$_2$), 1.40 (br m, 24 H, CH(CH_3)$_2$), 4.32 (br m, 8 H, CH(CH$_3$)$_2$), 5.07 (br m, 4 H, CH$_{BIAN}$), 6.31 (br m, 4 H, CH$_{BIAN}$), 6.53 (br m, 4 H, CH$_{BIAN}$), 7.05 ppm (br m, 12 H, *m-/p*-CH$_{Dipp}$); ^{13}C{^{1}H} NMR ([D$_7$]DMF, 300 K, 100.61 MHz) $\delta = 25.8$ (CH(CH_3)$_2$), 26.0 (CH(CH_3)$_2$), 27.9 (CH(CH_3)$_2$), 114.2 (br s, CH$_{BIAN}$), 118.0 (br s, CH$_{BIAN}$), 122.2 (br s, *meta*-C$_{Dipp}$), 123.2 (br s, *para*-C$_{Dipp}$), 128.1 (br s, CH$_{BIAN}$), 128.7 (br s, C$_{BIAN}$), 137.2 (br s, C$_{BIAN}$), 141.5 (br s, C$_{BIAN}$), 144.0 (br s, *o*-C$_{Dipp}$), 157.6 ppm (br s, *ipso*-C$_{Dipp}$), one ^{13}C NMR signal of a quarternary carbon atom of the BIAN ligand was not be detected, probably due to line broadening and signal overlap; ^{31}P{^{1}H} NMR ([D$_7$]DMF, 300 K, 161.98 MHz) $\delta = -45.9$ ppm (s); UV/Vis (THF): λ_{max} (ε) = 345 (24 200), 585 nm (35 200 L mol^{-1} cm^{-1}); NIR (THF): λ_{max} (ε) = 795 (14 000), 1135 nm (6500 L mol^{-1} cm^{-1}); elemental analysis calcd for C$_{80}$H$_{96}$N$_4$Co$_2$K$_2$O$_2$P$_4$ (1465.63): C 65.56, H 6.60, N 3.82; found: C 64.78, H 6.24, N 3.83. Crystals of [{K(OEt$_2$)}$_2${(BIAN)Co}$_2$(μ-η^4:η^4-P$_4$)] (**2b**) were obtained by storing a concentrated diethyl ether solution of **2a** at room temperature for one day; the spectroscopic data are identical to those of **2a**. Crystals of [K([18]crown-6)(MeCN)]$_2$[{(BIAN)Co}$_2$(μ-η^4:η^4-P$_4$)] (**2c**) were obtained by dissolving **2a** in acetonitrile, adding [18]crown-6, and diffusing diethyl ether into this solution over one day; characterization data for **2c**: ^{1}H NMR ([D$_7$]DMF, 300 K, 400.13 MHz) $\delta = 0.75$ (d, ^3J(H,H) = 6.0 Hz, 24 H, CH(CH_3)$_2$), 1.37 (d, ^3J(H,H) = 6.0 Hz, 24 H, CH(CH_3)$_2$), 3.62 (s, 48 H, [18]crown-6), 4.30 (br m, 8 H, CH(CH$_3$)$_2$), 5.07 (br m, 4 H, CH), 5.06 (br m, 4 H, CH), 6.28 (t, ^3J(H,H) = 7.4 Hz, 4 H, CH), 6.52 (br m, 4 H, CH), 6.98 (br m, 4 H, CH), 7.04 ppm (d, ^3J(H,H) = 7.4 Hz, 8 H, CH); ^{31}P{^{1}H} NMR ([D$_7$]DMF, 300 K, 161.98 MHz) $\delta = -44.0$ ppm (s); UV/Vis (THF): λ_{max} (ε) = 346 (24 500), 581 nm (36 000 L mol^{-1} cm^{-1}); elemental analysis calcd for C$_{100}$H$_{134}$N$_6$Co$_2$K$_2$O$_{12}$P$_4$·2 C$_2$H$_3$N (2012.75): C 62.01, H 7.01, N 5.56; found: C 61.46, H 6.65, N 5.19.

3a and **3b**: A solution of [Cp$_2$Fe]BAr$^F_4$ (55 mg, 0.053 mmol, 1.0 equiv) in THF (1 mL) was added dropwise to a suspension of **2a** (77 mg, 0.053 mmol, 1.0 equiv) in THF (3 mL). An immediate color change to dark blue was observed. After stirring the reaction mixture for 24 h, the solvent was removed and the residue was washed with *n*-hexane (7 mL). After extracting the residue with diethyl ether (8 mL), the filtrate was concentrated to 3 mL and stored at room temperature. Dark blue X-ray-quality crystals of **3a** formed upon storing for five days. Yield: 29 mg (41%); effective magnetic moment ([D$_8$]THF): $\mu_{eff} = 2.0(1)$ μ$_B$; ^{1}H NMR ([D$_8$]THF, 300 K, 400.13 MHz) $\delta = -0.9$ (br s), 0.8 (br s), 1.2 (br s, overlap with Et$_2$O), 3.4 (br s, overlap with Et$_2$O), 7.3 (br s), 17.4 (br s), 19.3 ppm (br s); UV/Vis (THF): λ_{max} (ε) = 342 (44 000), 575 nm (66 500 L mol^{-1} cm^{-1}); NIR (THF): λ_{max} (ε) = 777 (25 000), 1319 nm (2000 L mol^{-1} cm^{-1}); elemental analysis calcd for C$_{76}$H$_{90}$N$_4$Co$_2$KOP$_4$ (1356.44): C 67.30, H 6.69, N 4.13; found: C 68.29, H 6.73, N 4.11. Crystals of [K(dme)$_4$]

Acknowledgements

[1] Reviews: a) B. M. Cossairt, N. A. Piro, C. C. Cummins, *Chem. Rev.* **2010**, *110*, 4164; b) M. Caporali, L. Gonsalvi, A. Rossin, M. Peruzzini, *Chem. Rev.* **2010**, *110*, 4178; c) J. S. Figueroa, C. C. Cummins, *Dalton Trans.* **2006**, 2161; d) M. Peruzzini, L. Gonsalvi, A. Romerosa, *Chem. Soc. Rev.* **2005**, *34*, 1038; e) M. Peruzzini, R. Abdreimova, Y. Budnikova, A. Romerosa, O. J. Scherer, M. Sitzmann, *J. Organomet. Chem.* **2004**, *689*, 4319.

[2] Selected recent examples: a) S. Heinl, S. Reisinger, C. Schwarzmaier, M. Bodensteiner, M. Scheer, *Angew. Chem. Int. Ed.* **2014**, *53*, 7639; *Angew. Chem.* **2014**, *126*, 7769; b) S. Pelties, D. Herrmann, B. de Bruin, F. Hartl, R. Wolf, *Chem. Commun.* **2014**, *50*, 7014; c) S. Heinl, M. Scheer, *Chem. Sci.* **2014**, *5*, 3221; d) C. Schwarzmaier, A. Y. Timoshkin, G. Balázs, M. Scheer, *Angew. Chem. Int. Ed.* **2014**, *53*, 9077; *Angew. Chem.* **2014**, *126*,

9223; e) D. W. Agnew, C. E. Moore, A. L. Rheingold, J. S. Figueroa, *Angew. Chem. Int. Ed.* **2015**, *54*, 12673; *Angew. Chem.* **2015**, *127*, 12864; f) B. Pinter, K. T. Smith, M. Kamitani, E. M. Zolnhofer, B. L. Tran, S. Fortier, M. Pink, G. Wu, B. C. Manor, K. Meyer, *J. Am. Chem. Soc.* **2015**, *137*, 15247 – 15261.

[3] a) S. Charles, B. W. Eichhorn, A. L. Rheingold, S. G. Bott, *J. Am. Chem. Soc.* **1994**, *116*, 8077; b) S. Charles, J. C. Fettinger, S. G. Bott, B. W. Eichhorn, *J. Am. Chem. Soc.* **1996**, *118*, 4713; c) C. M. Knapp, J. S. Large, N. H. Rees, J. M. Goicoechea, *Chem. Commun.* **2011**, *47*, 4111.

[4] a) J. S. Figueroa, C. C. Cummins, *J. Am. Chem. Soc.* **2004**, *126*, 13916; b) W. W. Seidel, O. T. Summerscales, B. O. Patrick, M. D. Fryzuk, *Angew. Chem. Int. Ed.* **2009**, *48*, 115; *Angew. Chem.* **2009**, *121*, 121.

[5] a) M. V. Butovskiy, G. Balázs, M. Bodensteiner, E. V. Peresypkina, A. V. Virovets, J. Sutter, M. Scheer, *Angew. Chem. Int. Ed.* **2013**, *52*, 2972; *Angew. Chem.* **2013**, *125*, 3045; b) E. Mädl, G. Balázs, E. V. Peresypkina, M. Scheer, *Angew. Chem. Int. Ed.* **2016**, *55*, 7702 – 7707; *Angew. Chem.* **2016**, *128*, 7833 – 7838.

[6] a) T. Li, M. T. Gamer, M. Scheer, S. N. Konchenko, P. W. Roesky, *Chem. Commun.* **2013**, *49*, 2183; b) T. Li, N. Arleth, M. T. Gamer, R. Köppe, T. Augenstein, F. Dielmann, M. Scheer, S. N. Konchenko, P. W. Roesky, *Inorg. Chem.* **2013**, *52*, 14231.

[7] a) S. Yao, N. Lindenmaier, Y. Xiong, S. Inoue, T. Szilvási, M. Adelhardt, J. Sutter, K. Meyer, M. Driess, *Angew. Chem. Int. Ed.* **2015**, *54*, 1250; *Angew. Chem.* **2015**, *127*, 1266; b) S. Yao, T. Szilvási, N. Lindenmaier, Y. Xiong, S. Inoue, M. Adelhardt, J. Sutter, K. Meyer, M. Driess, *Chem. Commun.* **2015**, *51*, 6153.

[8] F. Spitzer, C. Graßl, G. Balázs, E. M. Zolnhofer, K. Meyer, M. Scheer, *Angew. Chem. Int. Ed.* **2016**, *55*, 4340; *Angew. Chem.* **2016**, *128*, 4412.

[9] B. M. Cossairt, M.-C. Diawara, C. C. Cummins, *Science* **2009**, *323*, 602.

[10] E. Urnèžius, W. W. Brennessel, C. J. Cramer, J. E. Ellis, P. von R. Schleyer, *Science* **2002**, *295*, 832.

[11] E.-M. Schnöckelborg, J. J. Weigand, R. Wolf, *Angew. Chem. Int. Ed.* **2011**, *50*, 6657; *Angew. Chem.* **2011**, *123*, 6787.

[12] a) K. Jonas, R. Mynott, C. Krüger, J. C. Sekutowski, Y.-H. Tsay, *Angew. Chem. Int. Ed. Engl.* **1976**, *15*, 767; *Angew. Chem.* **1976**, *88*, 808; b) K. Jonas, US patent 4169845, 1979.

[13] Related α-diimine complexes: a) M. Döring, E. Uhlig, T. Taldbach, *Z. Anorg. Allg. Chem.* **1991**, *600*, 163; b) W. W. Brennessel, J. E. Ellis, *Inorg. Chem.* **2012**, *51*, 9076; c) X. Wang, Y. Zhao, S. Gong, B. Liu, Q.-S. Li, J.-H. Su, B. Wu, X.-J. Yang, *Chem. Eur. J.* **2015**, *21*, 13302; d) C. Lichtenberg, L. Viciu, M. Vogt, R. E. Rodríguez-Lugo, M. Adelhardt, J. Sutter, M. M. Khusniyarov, K. Meyer, B. de Bruin, E. Bill, H. Grützmacher, *Chem. Commun.* **2015**, *51*, 13890; e) C. Lichtenberg, M. Adelhardt, T. L. Gianetti, K. Meyer, B. de Bruin, H. Grützmacher, *ACS Catal.* **2015**, *5*, 6230; f) C. Lichtenberg, L. Viciu, M. Adelhardt, J. Sutter, K. Meyer, B. de Bruin, H. Grützmacher, *Angew. Chem. Int. Ed.* **2015**, *54*, 5766; *Angew. Chem.* **2015**, *127*, 5858.

[14] Selected BIAN^0 complexes: a) D. P. Gates, S. A. Svejda, E. Oñate, C. M. Killian, L. K. Johnson, P. S. White, M. Brookhart, *Macromolecules* **2000**, *33*, 2320; b) J. O. Liimatta, B. Löfgren, M. Miettinen, M. Ahlgren, M. Haukka, T. T. Pakkanen, *J. Polym. Sci. Part A Polym. Chem.* **2001**, *39*, 1426; c) A. Paulovicova, U. El-Ayaan, K. Shibayama, T. Morita, Y. Fukuda, *Eur. J. Inorg. Chem.* **2001**, 2641; d) C. Fliedel, V. Rosa, C. I. M. Santos, P. J. Gonzalez, R. M. Almeida, C. S. B. Gomes, P. T. Gomes, M. A. N. D. A. Lemos, G. Aullón, R. Welter, T. Avilés, *Dalton Trans.* **2014**, *43*, 13041; e) T. Vaidya, K. Klimovica, A. M. LaPointe, I. Keresztes, E. B. Lobkovsky, O. Daugulis, G. W. Coates, *J. Am. Chem. Soc.* **2014**, *136*, 7213.

[15] Selected BIAN$^-$ complexes: a) I. L. Fedushkin, A. A. Skatova, V. A. Chudakova, V. K. Cherkasov, S. Dechert, H. Schumann, *Russ. Chem. Bull.* **2004**, *53*, 2142; b) I. L. Fedushkin, A. A. Skatova, S. Y. Ketkov, O. V. Eremenko, A. V. Piskunov, G. K. Fukin, *Angew. Chem. Int. Ed.* **2007**, *46*, 4302; *Angew. Chem.* **2007**, *119*, 4380; c) M. M. Khusniyarov, K. Harms, O. Burghaus, J. Sundermeyer, *Eur. J. Inorg. Chem.* **2006**, 2985; d) M. A. Ogienko, N. A. Pushkarevsky, A. I. Smolentsev, V. A. Nadolinny, S. Y. Ketkov, S. N. Konchenko, *Organometallics* **2014**, *33*, 2713; e) P. Mondal, H. Agarwala, R. D. Jana, S. Plebst, A. Grupp, F. Ehret, S. M. Mobin, W. Kaim, G. K. Lahiri, *Inorg. Chem.* **2014**, *53*, 7389.

[16] The dianionic BIAN^{2-} framework is typically observed in complexes with electropositive elements, for example, Mg and Al: a) I. L. Fedushkin, A. A. Skatova, V. A. Chudakova, G. K. Fukin, S. Dechert, H. Schumann, *Eur. J. Inorg. Chem.* **2003**, 3336; b) I. L. Fedushkin, A. N. Lukoyanov, A. N. Tishkina, M. O. Maslov, S. Y. Ketkov, M. Hummert, *Organome-*

tallics **2011**, *30*, 3628; d) I. L. Fedushkin, V. G. Sokolov, A. V. Piskunov, V. M. Makarov, E. V. Baranov, G. A. Abakumov, *Chem. Commun.* **2014**, *50*, 10108; e) H. Tsurugi, T. Saito, H. Tanahashi, J. Arnold, K. Mashima, *J. Am. Chem. Soc.* **2011**, *133*, 18673.

[17] M. J. Sgro, D. W. Stephan, *Dalton Trans.* **2010**, *39*, 5786.

[18] A very broad, irreversible oxidation wave was detected at $E_{pa} = -0.1$ V vs. Fc/Fc$^+$ and secondary processes at $E_{1/2} = -2.0$ V vs. Fc/Fc$^+$ were also observed. See the Supporting Information for further details.

[19] Selected publications on the solvatochromism of square planar LLCT complexes: a) R. Benedix, H. Hennig, H. Kunkely, A. Vogler, *Chem. Phys. Lett.* **1990**, *175*, 483; b) S. D. Cummings, R. Eisenberg, *Inorg. Chem.* **1995**, *34*, 2007; c) S. D. Cummings, R. Eisenberg, *J. Am. Chem. Soc.* **1996**, *118*, 1949; d) C.-T. Chen, S.-Y. Liao, K.-J. Lin, C.-H. Chen, T.-Y. J. Lin, *Inorg. Chem.* **1999**, *38*, 2734; e) C. J. Adams, N. Fey, M. Parfitt, S. J. A. Pope, J. A. Weinstein, *Dalton Trans.* **2007**, 4446.

[20] F. Kraus, J. C. Aschenbrenner, N. Korber, *Angew. Chem. Int. Ed.* **2003**, *42*, 4030; *Angew. Chem.* **2003**, *115*, 4162.

[21] a) A. Velian, C. C. Cummins, *Chem. Sci.* **2012**, *3*, 1003; b) C. Camp, L. Maron, R. G. Bergman, J. Arnold, *J. Am. Chem. Soc.* **2014**, *136*, 17652.

[22] Transition metal complexes with cyclo-P_4^{2-} ligands: a) O. J. Scherer, J. Vondung, G. Wolmershäuser, *Angew. Chem. Int. Ed. Engl.* **1989**, *28*, 1355; *Angew. Chem.* **1989**, *101*, 1395; b) M. Scheer, E. Herrmann, J. Sieler, M. Oehme, *Angew. Chem. Int. Ed. Engl.* **1991**, *30*, 969; *Angew. Chem.* **1991**, *103*, 1023; c) M. Scheer, U. Becker, J. C. Huffman, M. H. Chisholm, *J. Organomet. Chem.* **1993**, *461*, C1; d) see also reference [2d].

[23] a) M. Scheer, U. Becker, M. H. Chisholm, J. C. Huffman, F. Lemoigno, O. Eisenstein, *Inorg. Chem.* **1995**, *34*, 3117; b) M. D. Walter, J. Grunenberg, P. S. White, *Chem. Sci.* **2011**, *2*, 2120.

[24] An interaction with alkali metal cations can affect element-element bonds through several factors; a) J. Su, X.-W. Li, R. C. Crittendon, G. H. Robinson, *J. Am. Chem. Soc.* **1997**, *119*, 5471; b) N. Takagi, M. W. Schmidt, S. Nagase, *Organometallics* **2001**, *20*, 1646.

[25] The half-wave potential for the reduction of **4** ($E_{1/2}$(**4**→**3a**) = −1.26 V vs. Fc/Fc$^+$) is more positive than that for the complexes **E** and **F** ($E_{1/2}$(**E**→**G**) = −1.5 V vs. Fc/Fc$^+$, ($E_{1/2}$(**F**→**H**) = −1.4 V vs. Fc/Fc$^+$), indicating that the BIAN complexes are more easily reduced than the the corresponding nacnac compounds.[7]

[26] A possible explanation for the presence of two species **4a** and **4b** is that they are electromers.[27] In this case, the cobalt atoms and the P_4 unit might have different oxidation states, for example, P_4^{4-} + 2x Co^{III} for **2a** vs. P_4^{2-} + 2x Co^{II} for **4b**. The interconversion of electromeric **4a** and **4b** might have a substantial kinetic barrier, which might explain the two species do not show exchange phenomena in solution. Further investigations must reveal the physical oxidation state of the metal atoms in these complexes. Preliminary attempts to model **4a** and **4b** by broken-symmetry DFT calculations failed presumably due to the poor ability of standard DFT methods to properly describe the wavefunction of this type of molecule.

[27] T. Bally, *Nat. Chem.* **2010**, *2*, 165–166.

[28] a) O. J. Scherer, M. Swarowsky, G. Wolmershäuser, *Organometallics* **1989**, *8*, 841; b) S. Dürr, D. Ertler, U. Radius, *Inorg. Chem.* **2012**, *51*, 3904; c) B. Zarzycki, F. M. Bickelhaupt, U. Radius, *Dalton Trans.* **2013**, *42*, 7468.

[29] a) P. J. Chirik, K. Wieghardt, *Science* **2010**, *327*, 794–795; b) W. I. Dzik, J. I. van der Vlugt, J. N. H. Reek, B. de Bruin, *Angew. Chem. Int. Ed.* **2011**, *50*, 3356; *Angew. Chem.* **2011**, *123*, 3416.